

CP Violation Measurements at the Tevatron

M.R.J Williams

On behalf of the CDF and D0 Collaborations

*Department of Physics, Lancaster University, Bailrigg,
Lancaster LA1 4YB, England*



The two colliding beam experiments at the Tevatron proton-antiproton collider, CDF and D0, continue to publish world-leading measurements of CP Violation parameters in the B meson sector. I will present several recent results from both experiments, including measurements of direct CP violating parameters in decays of B_u^+ , B_d^0 and B_s^0 mesons; a new D0 measurement of a_{sl}^s using time-dependent analysis of $B_s \rightarrow \mu^+ \nu D_s^- X$ decays; and the latest Tevatron combination of the CP violating phase β_s , measured in the ‘golden mode’ $B_s \rightarrow J/\psi \phi$.

1 Introduction

While observational evidence strongly indicates that our universe is matter dominated, fundamental symmetry principles require that during the big-bang origin of the universe, exactly equal amounts of matter and antimatter were produced¹. Hence, current theoretical models postulate that a matter-antimatter asymmetry developed at some point in the history of the early universe. The pioneering physicist Andrei Sakharov postulated three necessary conditions for such a situation to occur. These are: Baryon number violation, a period of non-thermal-equilibrium, and sources of both C- and CP-symmetry violation². The Standard Model of particle physics includes some degree of CP-violation (CPV) as a result of a complex phase in the quark mixing (CKM) matrix. However, theoretical models strongly suggest that the level of Standard Model CPV is insufficient to describe the observed baryon asymmetry of the universe, in some cases by several orders of magnitude³. As such, it is important to investigate possible non-SM sources of CP violation.

CP violation studies in heavy-flavor physics can be divided broadly into three classes. Direct CPV occurs when the decay width of a process differs from that of its charge conjugate equivalent, for example in B meson decays to a final state f : $\Gamma(B \rightarrow f) \neq \Gamma(\bar{B} \rightarrow \bar{f})$. The

asymmetry of each such process is characterised by the quantity:

$$A_{CP}(B \rightarrow f) \equiv \frac{N(\bar{B} \rightarrow \bar{f}) - N(B \rightarrow f)}{N(\bar{B} \rightarrow \bar{f}) + N(B \rightarrow f)}, \quad (1)$$

where the convention is that the positive (negative) term in the numerator corresponds to the b (\bar{b}) quark process.

CP violation can also arise due to the mechanism of neutral B meson mixing, if the mass eigenstates are not pure CP states. In this case, the characteristic inequality is $\Gamma(\bar{B} \rightarrow f) \neq \Gamma(B \rightarrow \bar{f})$, i.e. there is an asymmetry a_{SL}^q in the decays of B mesons which have oscillated into their antiparticle prior to decay:

$$a_{SL}^q \equiv \frac{N(\bar{B}_q^0 \rightarrow f) - N(B_q^0 \rightarrow \bar{f})}{N(\bar{B}_q^0 \rightarrow f) + N(B_q^0 \rightarrow \bar{f})}. \quad (2)$$

Finally, in neutral B decays where the same final states are available with or without mixing, CP violation can be induced via interference between the mixed and unmixed process. An example of particular interest at the moment is the decay $B_s^0 \rightarrow J/\psi\phi$, since it enables a measurement of the parameter β_s , expected to be sensitive to the effects of physics beyond the Standard Model.

All three classes of CPV have been studied at the Tevatron experiments, and will be described in more detail in the remainder of this talk.

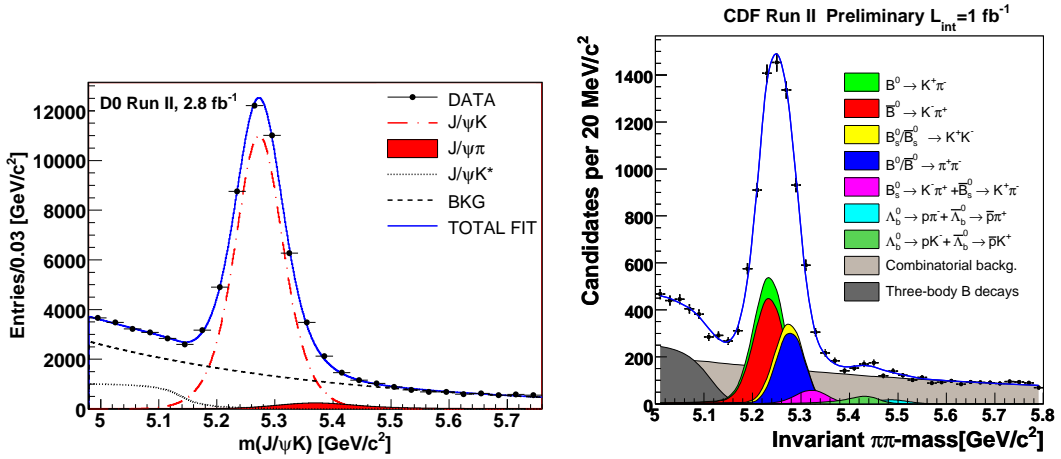
2 Experimental Environment

Both CDF⁸ and D0⁹ have been described in detail elsewhere. Both contain central tracking detectors within a magnetic field, surrounded by calorimetry, and with muon detectors placed furthest from the collision point. One of the strengths of the CDF detector relating to CPV measurements is an excellent momentum resolution, resulting from a large-volume tracking detector with many detection surfaces. In addition, the trigger system includes a dedicated displaced secondary-vertex trigger, which provides good efficiency for B hadron processes, in particular for fully hadronic decays where there is no lepton to provide the trigger signal. A benefit of the D0 detector is its excellent muon system, providing broad coverage over central and forward regions, and with thick shielding to reduce contamination from sources such as hadronic punch-through and beam spray. In addition, the magnet polarities in D0 are regularly reversed, which helps to mitigate detector-induced asymmetries, significantly reducing systematic uncertainties on asymmetry measurements.

3 Direct CP Violation

The D0 experiment has performed a search for direct CPV in $B^\pm \rightarrow J/\psi K^\pm(\pi^\pm)$ decays, using 2.8 fb^{-1} of data¹⁰. The parameter $A_{CP}(B^+ \rightarrow J/\psi K^+)$, defined according to Eq. (1), is predicted by the Standard Model to be small (~ 0.003). This is due to the smallness of the relative phase $\arg[-V_{cs}V_{cb}^*/V_{ts}V_{tb}^*]$ between tree-level and penguin diagrams in the $b \rightarrow sc\bar{c}$ transition. In contrast, the equivalent asymmetry $A_{CP}(B^+ \rightarrow J/\psi\pi^+)$, involving a $b \rightarrow dc\bar{c}$ transition, may be enhanced to order one percent as a result of the much larger phase $\arg[-V_{cd}V_{cb}^*/V_{td}V_{tb}^*]$.

After reconstructing the B^\pm mesons by appropriate combination of two muon objects (from $J/\psi \rightarrow \mu\mu$ decay) with a charged track, the signal fraction is optimised using a likelihood ratio method, combining several signal-sensitive variables into a single discriminant. Since charged kaons and pions cannot be distinguished on a particle-by-particle basis, the two decays are reconstructed collectively, and the relative number of each type is extracted from unbinned



(a) The $J/\psi K$ invariant mass distribution from the D0 measurement of $A_{CP}(B^\pm \rightarrow J/\psi K^\pm(\pi^\pm))$. Also shown is the result of an unbinned likelihood fit to the data.

(b) Invariant mass distribution $M(\pi\pi)$ from the CDF direct CPV search, shown with the fit to a combination of signal and background contributions.

Figure 1: Invariant mass plots used in searches for direct CPV by D0 (left) and CDF (right). In each case, the number of decays of each charge and type is determined from fits to the data, and used to extract A_{CP} .

maximum likelihood fits to the invariant mass $M(J/\psi K^\pm)$, as shown in Fig. 1(a). The fit includes contributions from $B \rightarrow J/\psi K$, $B \rightarrow J/\psi\pi$ (shifted upwards in mass, since the pion track is allocated the kaon mass), and partially reconstructed decays $B \rightarrow J/\psi K^*$.

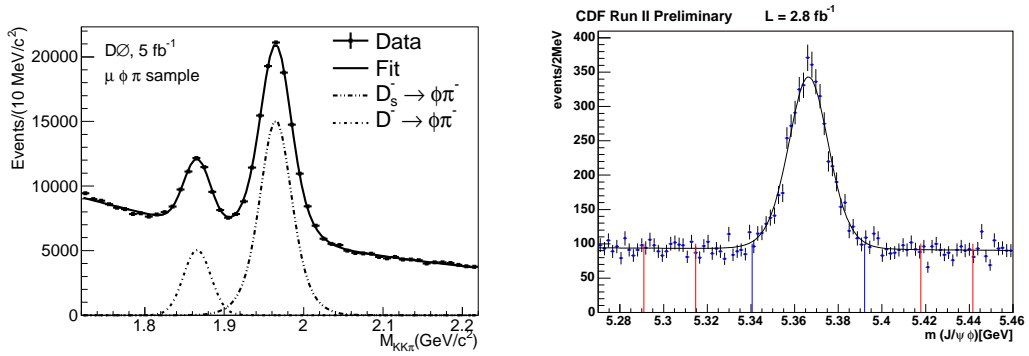
To disentangle possible detector effects from the CPV-induced asymmetry, the total data set is divided into eight sub-samples, according to the sign of the solenoid magnet polarity, the sign of the $J/\psi K$ system pseudorapidity, and the sign of the kaon charge. The number of $J/\psi K(\pi)$ candidates in each sample is extracted from the likelihood fit, and the results are used to solve a system of eight simultaneous equations which distinguish the true physics asymmetry from several possible sources of detector asymmetry. In addition, the contribution from kaon reconstruction asymmetry (caused by the difference in interaction cross-sections of K^+ and K^- in the detector) is measured directly in data, and used to correct for this effect. The resulting asymmetries are found to be:

$$A_{CP}(B^+ \rightarrow J/\psi K^+) = +0.0075 \pm 0.0061 \text{ (stat.)} \pm 0.0027 \text{ (syst.)} \quad (3)$$

$$A_{CP}(B^+ \rightarrow J/\psi\pi^+) = -0.09 \pm 0.08 \text{ (stat.)} \pm 0.03 \text{ (syst.)} \quad (4)$$

For the $J/\psi K$ case, this represents an improvement on the current world-average precision, while the $J/\psi\pi$ value shows competitive precision.

The CDF experiment has also performed a search for direct CPV, in decays $B_{(s)}^0 \rightarrow h^+ h'^-$ ($h, h' = K$ or π) using 1 fb^{-1} of data¹¹. Two sets of selection requirements are chosen such as to minimise the expected uncertainty of A_{CP} separately for low-yield and high-yield modes. The resulting mass distribution following application of the latter selection requirements is shown in Fig. 1(b). Despite the good mass resolution of $\sim 22 \text{ MeV}$, the various $B_{(s)}^0 \rightarrow h^+ h'^-$ channels are unresolved in this peak. Detailed Monte Carlo studies are performed to understand the expected $M(\pi\pi)$ contributions from different sources, which comprise the principal modes $B^0 \rightarrow \pi^+\pi^-$, $B^0 \rightarrow K^+\pi^-$ and $B_s^0 \rightarrow K^+K^-$, in addition to previously unobserved modes $B^0 \rightarrow K^+K^-$, $B_s^0 \rightarrow \pi^+K^-$, $\Lambda_b^0 \rightarrow p\pi^-$ and $\Lambda_b^0 \rightarrow pK^-$. Using a multi-dimensional unbinned maximum likelihood fit, the relative contributions of these modes is measured. After subtracting the



(a) Invariant mass plot for $D_s^- \rightarrow \phi\pi^-$, $\phi \rightarrow K^+K^-$ candidate events, one of two channels used to extract a_{SL}^s in decays $B_s^0 \rightarrow D_s^- \mu^+ \nu X$ at D0. Also shown is the fit to the data.

(b) Invariant mass plot for $B_s^0 \rightarrow J/\psi\phi$ events from the CDF measurement of ϕ_s . A neural net algorithm is used to optimise the signal selection.

Figure 2: Invariant mass distributions from CPV measurements made by D0 (right) and CDF (left).

asymmetry from kaon interaction effects, the following direct CPV parameters are extracted:

$$A_{CP}(B_s^0 \rightarrow K^- \pi^+) = +0.39 \pm 0.15 \text{ (stat.)} \pm 0.08 \text{ (syst.)} \quad (5)$$

$$A_{CP}(B^0 \rightarrow K^+ \pi^-) = -0.086 \pm 0.023 \text{ (stat.)} \pm 0.009 \text{ (syst.)}. \quad (6)$$

Equation (5) represents the first ever measurement of a CP asymmetry in the B_s^0 system.

4 CPV in Mixing: a_{sl}^s in $B_s \rightarrow \mu^+ \nu D_s^- X$ Decays

B_s^0 mixing was first observed at the Tevatron in 2006^{12,13}. It implies that the mass eigenstates, B_{sH} and B_{sL} , of the B_s^0 system are superpositions of the flavor eigenstates:

$$|B_{sH}\rangle = p |B_s\rangle - q |\bar{B}_s\rangle, \quad |B_{sL}\rangle = p |B_s\rangle + q |\bar{B}_s\rangle.$$

If $p \neq q$ then the mass eigenstates are not pure CP states, and the symmetry is violated. The experimental observables describing CPV in mixing are:

$$\phi_s = \arg(-M_{12}/\Gamma_{12}), \quad (7)$$

$$\Delta\Gamma_s = \Gamma_L - \Gamma_H \approx 2|\Gamma_{12}|\cos\phi_s, \quad (8)$$

$$\Delta M_s = M_H - M_L \approx 2|M_{12}|, \quad (9)$$

where $\Gamma_{H,L}$ and $M_{H,L}$ are the widths and masses of the heavy and light mass eigenstate, respectively, and Γ_{12} and M_{12} are off-diagonal components of the time-evolution matrix.

The flavor-specific semileptonic asymmetry a_{SL}^s as defined in Eq. 2 is sensitive to these parameters, according to the relation

$$a_{SL}^s = \frac{\Delta\Gamma_s}{\Delta M_s} \tan\phi_s. \quad (10)$$

D0 has recently performed a measurement of a_{SL}^s in decays $B_s^0 \rightarrow D_s^- \mu^+ \nu X$, with $D_s^- \rightarrow \phi\pi^-$, $\phi \rightarrow K^+K^-$ and $D_s^- \rightarrow K^*K^-$, $K^* \rightarrow K^+\pi^-$ ¹⁴. For each channel, the signal selection is optimised using a likelihood ratio method. The resulting D_s^- invariant mass distribution for the $\phi\pi^-$ case is shown in Fig. 2(a).

The rates of direct and mixed decays $\Gamma(B_s^0 \rightarrow \mu^\pm X)$ are sensitive to the parameter a_{SL}^s , according to the following relations (assuming no direct CPV):

$$\Gamma(B_s^0 \rightarrow \mu^- X) = N_f \cdot |A_f|^2 \cdot (\mathbf{1} - \mathbf{a}_{\mathbf{SL}}^s) \cdot e^{-\Gamma_s t} \cdot 1/2[\cosh(\Gamma_s t/2) - \cos(\Delta M_s t)] \quad (11)$$

$$\Gamma(B_s^0 \rightarrow \mu^+ X) = N_f \cdot |A_f|^2 \cdot (\mathbf{1} \quad) \cdot e^{-\Gamma_s t} \cdot 1/2[\cosh(\Gamma_s t/2) + \cos(\Delta M_s t)] \quad (12)$$

with similar expressions for the charge-conjugate decays. Without going into the details of these equations, which can be found elsewhere^{14,15}, they can be used to identify the most important aspects of the analysis. Firstly, the time-evolution of the decay rates means that a time-dependent analysis is needed to maximise sensitivity to a_{SL}^s ; in turn, this requires that the measured decay lengths be converted to the proper decay length through the use of so-called k-factors, which account for the missing neutrino energy. Secondly, only mixed decays are sensitive to a_{SL}^s , which implies that initial flavor tagging is required to reduce dilution from the non-mixed decays.

A multi-dimensional unbinned maximum likelihood fit is performed on the data, simultaneously fitting the visible proper decay length (VPDL) and its uncertainty, the mass of the D_s^- meson candidate, the predicted tagging dilution, and the value of the signal discriminant. The effect of different backgrounds is studied in detail using MC simulation, and fits to the mass distribution. In addition, detector asymmetries are accounted for in the fit, by including the regularly reversed toroid polarity as an additional input parameter. The results of the fit yield the following measurement of the semileptonic flavor-specific asymmetry:

$$a_{SL}^s = [-7.4 \pm 9.3 \text{ (stat.) } \begin{smallmatrix} +1.8 \\ -1.6 \end{smallmatrix} \text{ (syst.)}] \times 10^{-3}. \quad (13)$$

This is the most precise single measurement of a_{SL}^s , with precision currently dominated by the limited statistics. For reference, the Standard Model prediction is $a_{SL}^s = (0.0206 \pm 0.0057) \times 10^{-3}$.

5 β_s in $B_s \rightarrow J/\psi\phi$ Decays

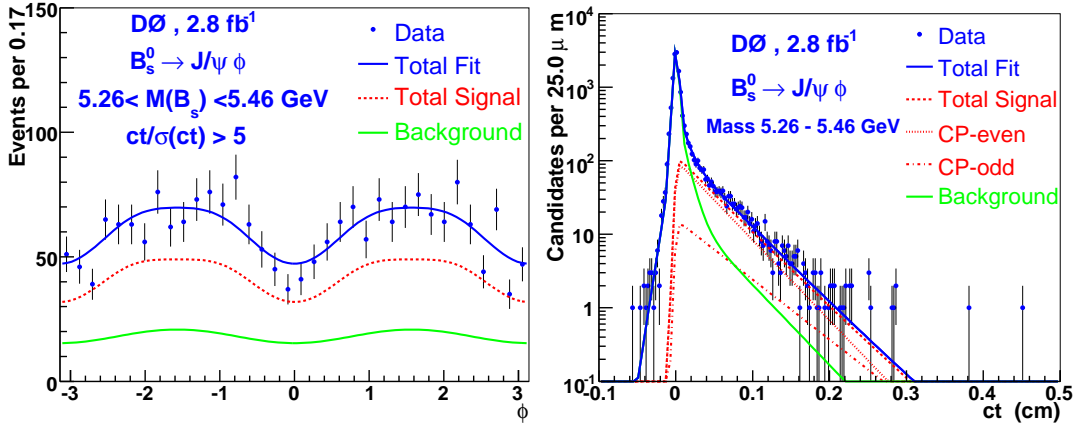
The third class of CPV in heavy-flavor physics arises due to the interference between direct and mixed decays to a common final state. For example, between the processes $B_s^0 \rightarrow J/\psi\phi$ and $B_s^0 \rightarrow \bar{B}_s^0 \rightarrow J/\psi\phi$. In this case, the parameter of interest is the relative phase between the mixing and decay amplitudes, $2\beta_s = -\arg[V_{tb}V_{ts}^*/V_{cb}V_{cs}^*]$. The SM predicts a value $2\beta_s = (0.04 \pm 0.01)$ rad, whereas new physics models can enhance this phase significantly. As such, this channel is an excellent probe for physics beyond the Standard Model.

Since both J/ψ and ϕ are vector particles, $J/\psi\phi$ is a superposition of CP-odd and CP-even final states. Angular analysis is thus required in order to separate the contributions from the CP eigenstates. In fact, there are three distinct polarisations: longitudinal, mutually parallel, and mutually perpendicular, associated with complex amplitudes $A_0(t)$, $A_{\parallel}(t)$, and $A_{\perp}(t)$, respectively. The differential decay rate can be written:

$$\begin{aligned} \frac{d^4\Gamma[B_s^0 \rightarrow J/\psi(\mu^+\mu^-)\phi(K^+K^-)]}{d\cos\theta d\phi d\cos\psi dt} &= f_1(\theta, \phi, \psi)|A_0(t)| + f_2(\theta, \phi, \psi)|A_{\parallel}(t)| \\ &+ f_3(\theta, \phi, \psi)|A_{\perp}(t)| + f_4(\theta, \phi, \psi)\Re[A_0^*(t)A_{\parallel}(t)] \\ &+ f_5(\theta, \phi, \psi)\Im[A_0^*(t)A_{\perp}(t)] + f_6(\theta, \phi, \psi)\Im[A_{\parallel}^*(t)A_{\perp}(t)], \end{aligned} \quad (14)$$

where (θ, ϕ, ψ) are characteristic decay angles of the event, and $f_i(\cdot)$ are well-defined functions omitted here for clarity. The complex amplitudes $A(t)$ depend on:

- Physical parameters $\Delta\Gamma_s$, ΔM_s , β_s , $\bar{\tau}_s$ (mean lifetime of B_s^0 system);
- The initial flavor of the B_s^0 meson;



(a) Distribution and fit of ϕ , one of the three characteristic event angles.

(b) Distribution and fit of the B_s^0 lifetime

Figure 3: D0 results (in two variables) of the likelihood fit over the time-dependent angular distribution of decays $B_s^0 \rightarrow J/\psi\phi$, used to measure the physical parameters of the system, such as ϕ_s and $\Delta\Gamma_s$.

- The boundary values $A(t=0)$;
- Phases of complex amplitudes δ_1 and δ_2 .

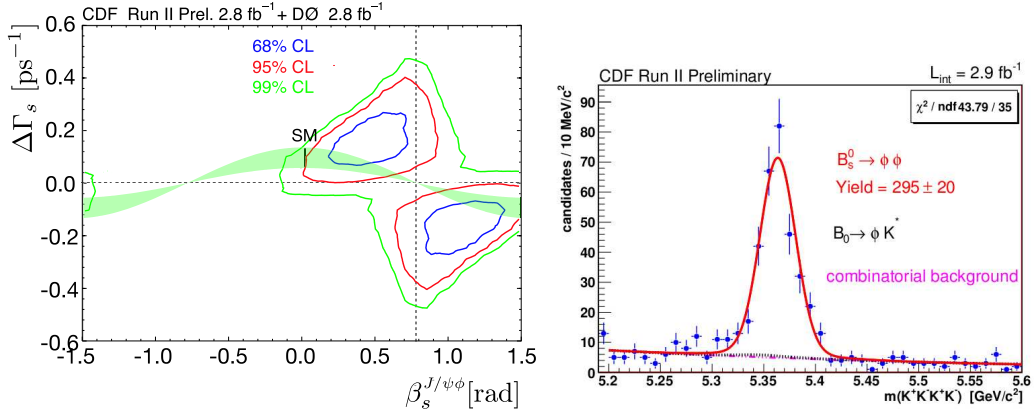
Both CDF¹⁶ and D0¹⁷ have performed recent measurements of β_s in the $J/\psi\phi$ channel, each using 2.8 fb^{-1} of data. The analysis strategy is the same for both experiments: a likelihood fit is performed over the time-dependent angular distribution. As in the a_{SL}^s measurement, flavor tagging is used to provide additional sensitivity. The effectiveness of tagging is characterised by the power ϵD^2 , where ϵ is the efficiency (fraction of total events which are tagged) and D is the dilution (fraction of correct tags minus fraction of incorrect tags). For the CDF (D0) analysis, a power of 1.8% (2.5%) is reported for opposite-side tagging. Another requirement is that the angular acceptances and efficiencies be well-modelled; simulations are used for this purpose.

Events are selected using a cut-based (D0) or neural net (CDF) selection, with yields of around 2K and 3K events respectively. Figure 2(b) shows the resulting $J/\psi\phi$ invariant mass distribution from the CDF analysis. Following event selection, flavor-tagging, and modelling of detector effects, the multi-dimensional likelihood fit is performed. Figure 3(a) shows the D0 fit results for ϕ , one of the three event angles in Eq. (14), while Fig. 3(b) shows the associated fit result for the lifetime.

Results are presented in terms of the two-dimensional likelihood contours in the $(\beta_s, \Delta\Gamma_s)$ plane, which correct for systematic uncertainties and the effects of non-Gaussian uncertainties (using pseudo-experiments). The results from CDF and D0 are in agreement, and have been combined by the Tevatron Averaging Group¹⁸. The results are shown in Fig. 4(a), and are inconsistent with the SM prediction at a statistical level of 2.12σ . The ambiguities apparent in Fig. 4(a) are a result of symmetries in the complex amplitudes under certain transformations of β_s and $\Delta\Gamma_s$. New results in this channel from both experiments are expected for the Summer 2010 conference season.

5.1 The Charmless Analogue: $B_s \rightarrow \phi\phi$

CDF have performed a search for $B_s \rightarrow \phi\phi$ decays using 2.9 fb^{-1} of data. This is the charmless analogue of the golden $J/\psi\phi$ mode. However, the dominant Standard Model process is the $b \rightarrow s$ penguin diagram, and therefore the relative branching fraction is expected to be small



(a) Combination of CDF and D0 measurements (2.8 fb^{-1}) of the 2D likelihood contours in $(\beta_s, \Delta\Gamma_s)$, obtained from the time-dependent angular analysis of $B_s^0 \rightarrow J/\psi\phi$ decays. The data is inconsistent with the Standard Model prediction at a statistical level of 2.1σ .

(b) Invariant mass distribution of $B_s^0 \rightarrow \phi\phi$ decays, the charmless analogue of $B_s^0 \rightarrow J/\psi\phi$. The fit to data allows the relative branching fractions of the two decays to be measured.

Figure 4: CP Violation in the interference between mixing and decay amplitudes of $B_s^0 \rightarrow J/\psi\phi$ decays is expressed in terms of the $(\beta_s, \Delta\Gamma_s)$ contour plot (left). The equivalent charmless decay $B_s^0 \rightarrow \phi\phi$ is suppressed in the Standard Model, quantified by the relative branching ratio measured by CDF (right).

with respect to $J/\psi\phi$. In principal, a measurement of the CP-violating phase β_s in this channel different from the corresponding phase in $J/\psi\phi$ (tree-dominated) would be an indication of New Physics in penguin-decays, in addition to any observations in mixing.

Events are selected in the final state $K^+K^-K^+K^-$ according to requirements on a number of discriminating variables, optimised separately to maximise $S/\sqrt{S+B}$, where S (B) is the number of signal (background) events in the region of the mass peak. The resulting invariant mass distribution is shown in Fig. 4(b); the signal contribution is fitted with a double-Gaussian function, with $N(\phi\phi) = 295 \pm 20$ candidates; the background is modelled by an exponential function. Using the same selection criteria, the equivalent mass distribution for the $J/\psi\phi$ final state is found to contain 1766 ± 48 candidates. In these fits, contributions from mis-identified decays to $J/\psi K^*$ and ϕK^* are taken into account using input from simulation. The relative branching ratio for the two B_s^0 decays is then determined using the formula:

$$\frac{\mathcal{B}(B_s^0 \rightarrow \phi\phi)}{\mathcal{B}(B_s^0 \rightarrow J/\psi\phi)} = \frac{N_{\phi\phi}}{N_{J/\psi\phi}} \cdot \frac{\mathcal{B}(J/\psi \rightarrow \mu\mu)}{\mathcal{B}(\phi \rightarrow K^+K^-)} \cdot \frac{\varepsilon_{J/\psi\phi}}{\varepsilon_{\phi\phi}} \cdot \varepsilon_{\mu}. \quad (15)$$

The branching fractions of $J/\psi \rightarrow \mu\mu$ and $\phi \rightarrow K^+K^-$ are taken from the Particle Data Group. The ratio of selection efficiencies $\varepsilon_{J/\psi\phi}/\varepsilon_{\phi\phi}$ is measured in simulation, and is found to be $0.939 \pm 0.030 \pm 0.009$; this value is close to unity because all events are required to satisfy a displaced secondary vertex trigger, with no input from muon-based triggers. The additional factor ε_{μ} accounts for the fact that, in the $J/\psi\phi$ case, at least one muon is required to be identified by the muon detector; it is measured in data to be 0.8695 ± 0.0044 . Putting together all the numbers, the relative and absolute branching ratios are found to be:

$$\frac{\mathcal{B}(B_s^0 \rightarrow \phi\phi)}{\mathcal{B}(B_s^0 \rightarrow J/\psi\phi)} = [1.78 \pm 0.14 \text{ (stat.)} \pm 0.20 \text{ (syst.)}] \% \quad (16)$$

$$\mathcal{B}(B_s^0 \rightarrow \phi\phi) = [2.40 \pm 0.21 \text{ (stat.)} \pm 0.27 \text{ (syst.)} \pm 0.82 \text{ (BR)}] \times 10^{-5}. \quad (17)$$

The absolute branching fraction is in agreement with current theoretical predictions, although the uncertainties on these values are large¹⁹.

6 Conclusions

CP Violation in B hadron physics is currently generating excitement in the particle physics community. Both CDF and D0 are becoming sensitive to small deviations from the Standard Model predictions, as a result of a rapidly increasing dataset, very mature and stable accelerator and detector complex, and improved use of innovative analysis tools, such as multivariate selection techniques. While disagreement with the SM is only at a low-level (around 2σ) at the moment, consistent deviations are observed in multiple independent measurements, from two independent experiments. As such, it is important that the experimental precision continues to improve, to increase the statistical power to differentiate between the SM predictions and possible New Physics contributions.

In addition to the analyses described here, there are several other studies ongoing, such as a measurement of $\Gamma_s^{\text{CP-even}} - \Gamma_s^{\text{CP-odd}}$ in decays $B_s^0 \rightarrow D_s^{(*)} D_s^{(*)}$, and an updated result in the dimuon asymmetry measurement, which is sensitive to a_{SL}^s and ϕ_s . In these early days of the LHC experiment, our goal at the Tevatron is to continue to produce high quality measurements, build on our legacy as a discovery machine, and set some tough standards to match.

References

1. E. W. Kolb and M. S. Turner, “The Early Universe”, Addison-Wesley (1990).
2. A. D. Sakharov, “Violation of CP invariance, C asymmetry, and baryon asymmetry of the universe”, *Journal of Experimental and Theoretical Physics* **5**, 24-27 (1967).
3. P. Huet and E. Sather, “Electroweak Baryogenesis and Standard Model CP Violation”, *Phys. Rev. D* **51**, 625-648 (1994).
4. C. Jarlskog in *CP Violation*, ed. C. Jarlskog (World Scientific, Singapore, 1988).
5. L. Maiani, *Phys. Lett. B* **62**, 183 (1976).
6. J. D. Bjorken and I. Dunietz, *Phys. Rev. D* **36**, 2109 (1987).
7. C. D. Buchanan *et al.*, *Phys. Rev. D* **45**, 4088 (1992).
8. D. E. Acosta *et al.* [CDF Collaboration], *Phys. Rev. D* **71**, 032001 (2005).
9. V. M. Abazov *et al.* [D0 Collaboration], *Nucl. Instrum. Methods A* **565**, 463 (2006).
10. V. M. Abazov *et al.* [D0 Collaboration], *Phys. Rev. Lett.* **100**, 211802 (2008).
11. D. E. Acosta *et al.* [CDF Collaboration], *Phys. Rev. Lett.* **94**, 122001 (2005); Update in CDF Public Note 8579.
12. V. M. Abazov *et al.* [D0 Collaboration], *Phys. Rev. Lett.* **97**, 021802 (2006).
13. A. Abulencia *et al.* [CDF Collaboration], *Phys. Rev. Lett.* **97**, 242003 (2006).
14. V. M. Abazov *et al.* [D0 Collaboration], arXiv:0904.3907 [hep-ex] (accepted by *Phys. Rev. D*).
15. K. Anikeev *et al.*, “ B physics at the Tevatron: Run II and beyond”, arXiv:hep-ph/0201071.
16. T. Aaltonen *et al.* [CDF Collaboration], *Phys. Rev. Lett.* **100**, 161802 (2008); Update in CDF Public Note 9458.
17. V. M. Abazov *et al.* [D0 Collaboration], *Phys. Rev. Lett.* **101**, 241801 (2008).
18. CDF Public Note 9787; D0 Public Note 5928.
19. M. Beneke, J. Rohrer and D. Yang, *Nucl. Phys. B* **774**, 64 (2007).